

This is a repository copy of *A comparative analysis of fibroblast growth factor receptor signalling during Xenopus development*.

White Rose Research Online URL for this paper:

<https://eprints.whiterose.ac.uk/157072/>

Version: Published Version

Article:

Isaacs, Harry Victor orcid.org/0000-0001-7825-536X and Brunsdon, Hannah Rebecca (2020) *A comparative analysis of fibroblast growth factor receptor signalling during Xenopus development*. *Biology of the Cell*. pp. 1-13. ISSN 0248-4900

<https://doi.org/10.1111/boc.201900089>

Reuse

Items deposited in White Rose Research Online are protected by copyright, with all rights reserved unless indicated otherwise. They may be downloaded and/or printed for private study, or other acts as permitted by national copyright laws. The publisher or other rights holders may allow further reproduction and re-use of the full text version. This is indicated by the licence information on the White Rose Research Online record for the item.

Takedown

If you consider content in White Rose Research Online to be in breach of UK law, please notify us by emailing eprints@whiterose.ac.uk including the URL of the record and the reason for the withdrawal request.

A comparative analysis of fibroblast growth factor receptor signalling during *Xenopus* development

Hannah Brunsdon²  and Harry V. Isaacs¹ 

Department of Biology, University of York, York YO10 5DD, UK

Background Information. The fibroblast growth factor (FGF) signalling system of vertebrates is complex. In common with other vertebrates, secreted FGF ligands of the amphibian *Xenopus* signal through a family of four FGF receptor tyrosine kinases (fgfr1, 2, 3 and 4). A wealth of previous studies has demonstrated important roles for FGF signalling in regulating gene expression during cell lineage specification in amphibian development. In particular, FGFs have well-established roles in regulating mesoderm formation, neural induction and patterning of the anteroposterior axis. However, relatively little is known regarding the role of individual FGFRs in regulating FGF-dependent processes in amphibian development. In this study we make use of synthetic drug inducible versions of *Xenopus* Fgfr1, 2 and 4 (iFgfr1, 2 and 4) to undertake a comparative analysis of their activities in the tissues of the developing embryo.

Results. We find that *Xenopus* Fgfr1 and 2 have very similar activities. Both Fgfr1 and Fgfr2 are potent activators of MAP kinase ERK signalling, and when activated in the embryo during gastrula stages regulate similar cohorts of transcriptional targets. In contrast, Fgfr4 signalling in naïve ectoderm and neuralised ectoderm activates ERK signalling only weakly compared to Fgfr1/2. Furthermore, our analyses indicate that in *Xenopus* neural tissue the Fgfr4 regulated transcriptome is very different from that of Fgfr1.

Conclusion and significance. We conclude that signalling downstream of Fgfr1 and 2 regulates similar processes in amphibian development. Interestingly, many of the previously identified canonical transcriptional targets of FGF regulation associated with germ layer specification and patterning are regulated by Fgfr1/Fgfr2 signalling. In contrast, the downstream consequences of Fgfr4 signalling are different, although roles for Fgfr4 signalling in lineage specification and anteroposterior patterning are also indicated.



Additional supporting information may be found online in the Supporting Information section at the end of the article.

Introduction

The vertebrate fibroblast growth factor (FGF) signalling network is complex. The human genome

encodes 22 FGF family proteins (Itoh and Ornitz, 2008; Ornitz and Itoh, 2015). FGF1-9 and 19–23 are secreted proteins, and fulfil either paracrine or endocrine functions by activating a family of four cell surface receptor tyrosine kinases (FGFR 1, 2, 3 and 4). Another subgroup of FGFs (FGF11–14) are not secreted, do not bind to FGFRs and have intracellular functions (Goldfarb, 2005; Itoh and Ornitz, 2008; Ornitz and Itoh, 2015).

FGFs mediate a broad range of biological functions during development, including the regulation of cell growth, survival and differentiation, reviewed (Böttcher et al., 2005; Dorey and Amaya, 2010; Pownall and Isaacs, 2010). The specific effects of FGF signalling are often dependent on developmental stage

¹To whom correspondence should be addressed (email: harry.isaacs@york.ac.uk)

²Current address: MRC Human Genetics Unit, Institute of Genetics and Molecular Medicine, University of Edinburgh, United Kingdom

Key words: cellular differentiation, development, growth factors.

Abbreviations: BMP, bone morphogenetic protein; dp-ERK, diphospho-extracellular signal-regulated kinase; ERK, extracellular signal-regulated kinase; FPKM, Fragments Per Kilobase of transcript per Million; Fgf, fibroblast growth factor; Fgfr, fibroblast growth factor receptor; GO, gene ontology; iFgfr, inducible; JAK, janus kinase; MAP, mitogen activated protein; MAPK, mitogen activated protein kinase; MBT, mid-blastula transition; NAM, normal amphibian medium; PLC- γ , phospholipase c gamma; PI3-kinase, Phosphoinositide 3-kinase; PKC, protein kinase c; STAT, signal transducer and activator of transcription protein.

and/or cell-type and understanding the mechanisms that regulate the diversity and specificity of FGF action remains a challenge.

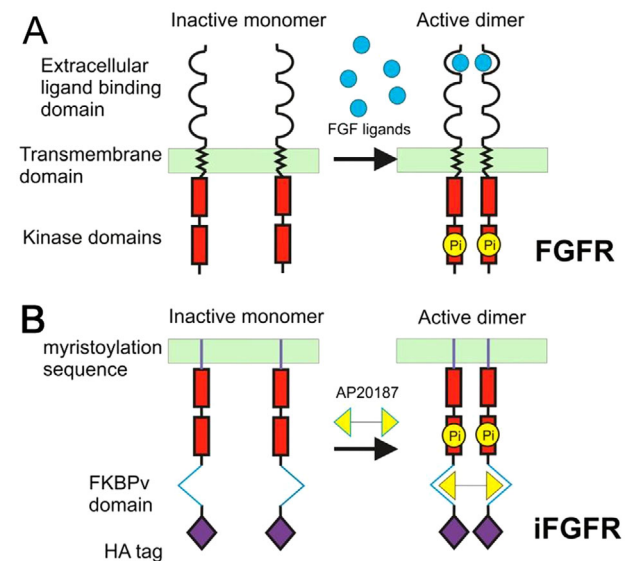
There is evidence for specificity in the downstream effects resulting from the activation of individual FGFRs during development (Umbhauer et al., 2000; Carballada et al., 2001; Yamagishi and Okamoto, 2010). Each of the receptors activate a similar set of intracellular signal transduction pathways, including the PLC- γ , PI3-kinase, PKC, JAK/STAT and MAP kinase pathways, reviewed (Brewer et al., 2016). However, there is diversity in the degree to which each pathway is activated by a given FGFR. It has been reported that FGFR1 activates MAP kinase ERK more strongly than does FGFR3 and FGFR4. This has been suggested as a possible mechanism underlying the different responses of PC12 cells to the activation of FGFR1, 3 and 4 signalling (Raffioni et al., 1999) and the weakened mitogenic response of Baf3 cells to FGFR3 or FGFR4 activation compared to FGFR1 or FGFR2 (Ornitz et al., 1996).

In the present study, we have investigated the effects of signalling by individual FGFRs in the amphibian *Xenopus*. The complement of FGF ligands and receptors in *Xenopus* is similar to that of mammals, with *fgfr1*, 2, 3 and 4 present, together with 20 ligands annotated in the *Xenopus laevis* genome (Suzuki et al., 2017). Previous studies in *Xenopus* have focussed on the role that FGF signalling plays in regulating gene transcription during germ layer specification and neural development, reviewed (Böttcher et al., 2005; Dorey and Amaya, 2010; Pownall and Isaacs, 2010). However, relatively little is currently known about how signalling downstream of individual FGFRs contributes to the overall FGF regulatory network in early amphibian development, particularly during neural development.

We have previously characterised the use of a drug inducible form of murine FGFR1 (iFGFR1) for studying FGF signalling in development. iFGFRs consist of the membrane anchored intracellular domain from an FGFR protein, fused to the ligand binding domain of the synthetic dimerisation agent AP20187 (Figure 1) (Welm et al., 2002; Pownall et al., 2003b). Analogous to FGF ligand-driven dimerisation of wild-type FGFRs, addition of the membrane soluble dimerising agent to cells expressing an iFgfr leads to rapid homodimerisation and activation of downstream signal transduction. Importantly,

Figure 1 | Schematic diagram of iFgfrs compared to endogenous FGFRs

Panel (A) is a schematic diagram of a wild type FGFR. FGF ligands bind to extracellular Ig-like domains. Receptor monomers are drawn into close proximity, and transphosphorylation of the kinase domains (red) activate downstream FGF signalling pathways. Panel (B) shows an iFgfr tethered to the cell membrane by a myristoylation domain. The 1 μ M AP20187 added to culture medium binds to the FKBPv domain, bringing the kinase domains as in (A). The HA tag tethered to the FKBPv domain enables immunodetection of the construct.



tantly, iFgfrs lack their extracellular ligand binding domains, and are not activated by endogenous FGF ligands. Thus, iFgfrs are a means to analyse the effects resulting from specifically activating signalling downstream of each FGFR, in the absence of the complexities that result from the promiscuous receptor binding properties of individual FGF ligands.

In the present study, we have developed drug inducible forms of *Xenopus* FGF receptors 1, 2 and 4 (iFgfr1, 2 and 4) to determine whether the different Fgfrs mediate distinct biological activities after mesoderm induction, and during gastrula stages. Using iFgfr constructs expressed in *Xenopus* embryonic tissues, we show that iFgfr1 and iFgfr2 both strongly activate MAP kinase ERK, whereas iFgfr4 is a relatively weak activator. Similarly, we find that iFgfr1 and iFgfr2 regulate similar patterns of gene expression in whole embryos during

gastrula stages. In contrast, we find that iFgfr1 and iFgfr4 signalling in neuralised tissue explants elicits distinct patterns of gene expression. We conclude that Fgfr1 and Fgfr2 mediate a common set of processes during early amphibian development, and these are distinct from those mediated by Fgfr4.

Results and discussion

iFgfrs have differing abilities to activate MAP kinase ERK

The present study was aimed at investigating FGFR gene regulatory pathways during gastrula stages. An analysis of temporal expression profiles of *Xenopus laevis* Fgfrs based on published RNA-Seq data (Session et al., 2016), indicates that expression levels of *fgfr1*, 2 and 4 are elevated from late blastula stages through to the end of gastrulation. However, *fgfr3* shows low-level maternal expression, which declines at the start of gastrulation and only begins to rise again at the early neurula stage (Supporting Information Figure 1). As a result, we have not included *fgfr3* in our study.

Treatment of blastula stage animal hemisphere explants (henceforth animal cap explants) with several different FGF ligands induces mesodermal cell fate in this pluripotent cell population (Slack et al., 1987; Isaacs et al., 1992; Song and Slack, 1996; Lombardo et al., 1998; Fletcher et al., 2006), accompanied by activation of MAP kinase signalling (LaBonne et al., 1995; Christen and Slack, 1999b). We used animal cap explants to investigate the ability of each iFgfr to activate MAP kinase signalling. Western blotting shows that the induction of signalling by addition of the dimerising agent AP20187 to iFgfr1, 2 and 4 injected animal cap explants increased levels of activated diphospho-ERK (dp-ERK) relative to uninduced control explants (Figure 2A). The most robust increases occurred with iFgfr1 and 2, with only a modest upregulation resulting from iFgfr4 activation. We note that the strong phosphorylation of ERK following activation of iFgfr1 and 2 reproducibly led to a concomitant reduction in the level of total ERK detected. The less potent activation of ERK by iFgfr4 did not have this effect. It is not clear whether this is genuine downregulation of total ERK levels or represents a masking of the total ERK epitope in the phosphorylated form of the protein.

Immunohistochemical analysis of the spatial distribution dp-ERK reactivity in control uninjected

embryos shows that ERK activation is restricted to known areas of endogenous FGF signalling in the equatorial region of the embryo (Figure 2B). In keeping with previous studies dp-ERK immunoreactivity is not detected in animal hemisphere cells (see control uninjected and iFgfr injected embryos in Figure 2C) (Christen and Slack, 1999b; Branney et al., 2009).

In contrast, Figure 2C shows ectopic dp-ERK staining in the animal hemisphere after animal hemisphere injections of iFgfr constructs and subsequent activation with AP20187 for 2 h. Activation of iFgfr1 and iFgfr2 resulted in robust and widespread dp-ERK immunostaining, whereas induction of iFgfr4 signalling led to weaker and less widespread dp-ERK activation. We conclude that Fgfr4 is a weak activator of MAP kinase signalling compared to both Fgfr1 and 2.

Signalling by different iFgfrs has distinct effects on tissue morphogenesis

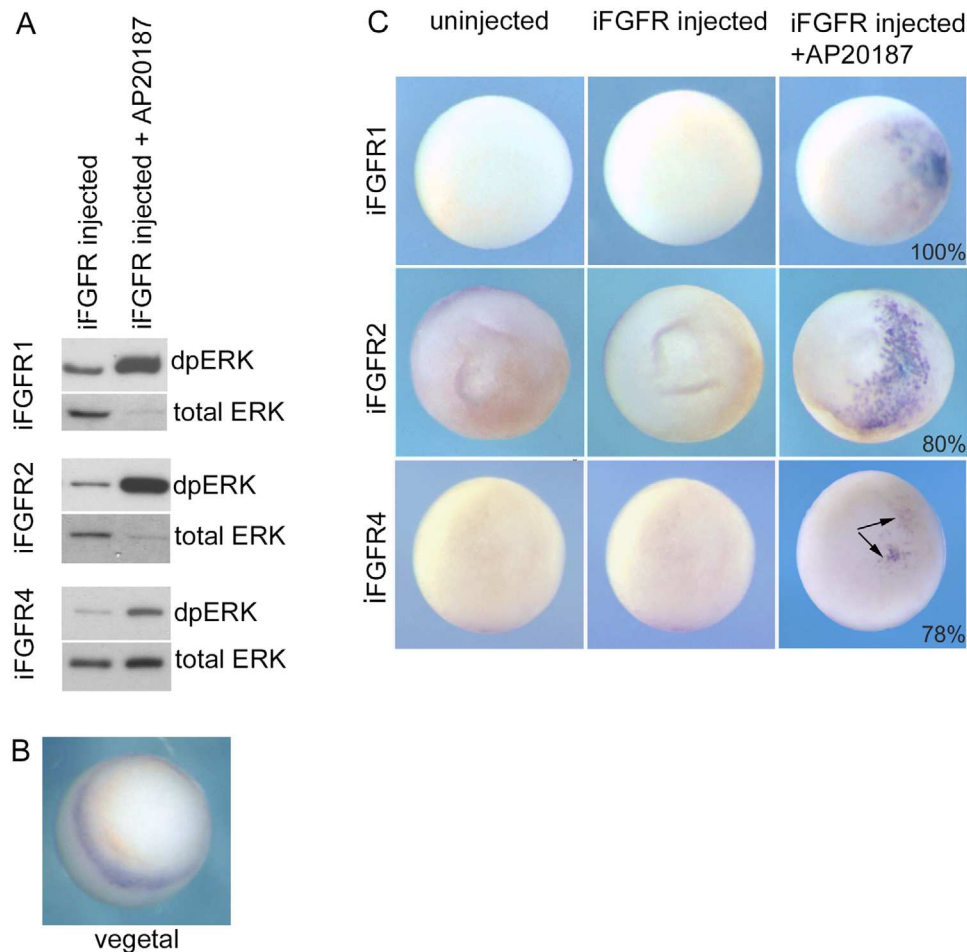
Animal cap explants treated with mesoderm-inducing FGF ligands elongate during gastrula and neurula stages, as the induced tissues undergo cell movements mimicking the morphogenetic movements of the mesoderm during normal development (Slack et al., 1988). Figure 3A shows that activation of iFgfr1 and iFgfr2 signalling induced tissue explant elongation, whereas iFgfr4 signalling did not.

Injection of synthetic FGF mRNAs into zygotes causes the rapid accumulation of FGF protein during cleavage and blastula stages, and results in catastrophic disruption of development due to the induction of ectopic mesodermal tissues during mid- to late-blastula stages (Isaacs et al., 1994). To investigate the effects of FGF overexpression in post-blastula stages plasmid-based, promoter driven expression of FGF ligands has been used in number of studies (Isaacs et al., 1994; Pownall et al., 1996). This methodology restricts ectopic FGF expression until after activation of zygotic transcription at the mid-blastula transition (MBT). Post-MBT FGF overexpression results in a penetrant posteriorised phenotype, characterised by loss of anterior structures, including eyes and anterior neural domains (Isaacs et al., 1994; Pownall et al., 1996).

Here we have investigated the effects on larval phenotype when signalling by different iFgfrs is activated only from early gastrula stages onwards. *ifgfr1*, 2 and 4 were injected into *Xenopus laevis* embryos and AP20187 added at gastrula stage 10.5. Figure 3B

Figure 2 | Effects of iFgfr activation on MAP kinase signalling

(A) Western blot showing levels of diphospho-ERK (dpERK) and total ERK in animal cap explants from embryos injected with 20 pg *iFgfr1*, *iFgfr2* or *iFgfr4* mRNA. Explants were removed at blastula stage 8 and treated with AP20187 for 2 h. **(B)** Whole mount immunohistochemical detection (vegetal view) of dpERK in the marginal zone of a gastrula stage 10 control embryo. **(C)** Whole mount immunohistochemical detection (animal view) of dpERK in animal hemisphere cells of gastrula stage 10 control embryos and embryos injected with 20pg *iFgfr1*, *iFgfr2* or *iFgfr4* mRNA (plus or minus 1 μ M AP20187 treatment from blastula stage 8). Percentages of explants from a representative experiment exhibiting the presented phenotype are indicated.

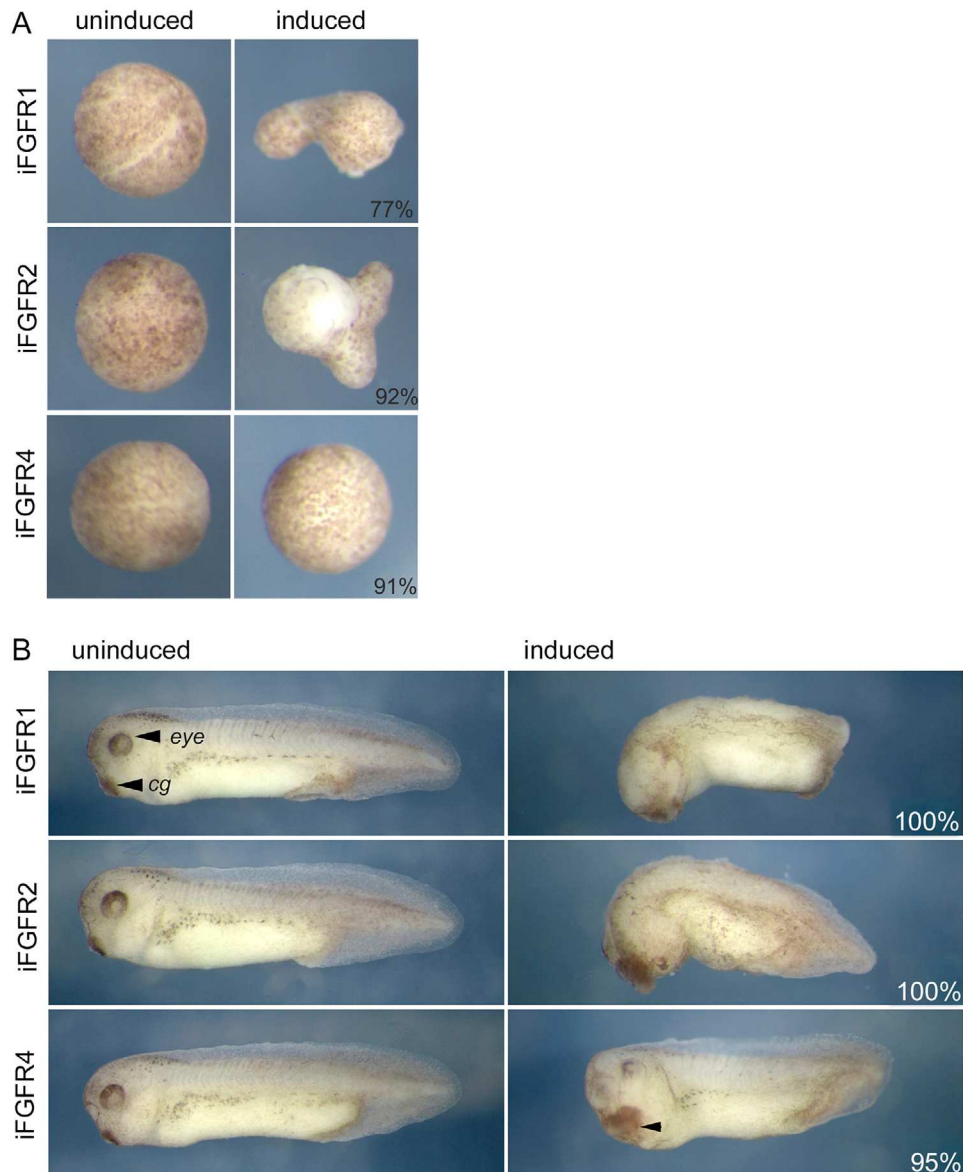


shows that uninjected control embryos, and those injected with *ifgfrs* but not treated with AP20187, developed normally. However, activation of *iFgfr1* or *iFgfr2* signalling caused severe defects, with reduced head development, including loss of eyes, cement gland and defective anteroposterior elongation relative to controls. These phenotypes are similar to those reported to arise from post-MBT activation of FGF4 signalling (Isaacs et al., 1994; Pownall et al., 1996). *iFgfr4* activation produced penetrant, but

milder defects than either *iFgfr1* or *iFgfr2* activation. Eyes were typically underdeveloped and this was accompanied by failure to properly elongate along the anteroposterior axis. Unlike with *iFgfr1* and *iFgfr2* activation, in *iFgfr4*-activated embryos the cement gland was not typically lost and was sometimes enlarged. We conclude that ectopic activation of *Fgfr1* and *Fgfr2* signalling has similar effects on morphogenesis of the *Xenopus* embryo, which are distinct from those resulting from *Fgfr4* signalling.

Figure 3 | Effects of iFgfr activation on tissue morphogenesis

Panel (A) compares the appearance of animal caps from embryos injected with 20pg *ifgfr1*, *ifgfr2* or *ifgfr4* mRNA \pm 1 μ M AP20187. AP20187 treatments occurred from blastula stage 8 until late neurula stage 18. Percentages of explants from a representative experiment exhibiting the presented phenotype are indicated, *ifgfr1*, $n = 9$, *ifgfr2* $n = 12$, *ifgfr4*, $n = 11$. Panel (B) compares the appearance at the tailbud stage of embryos injected with 20pg *ifgfr1*, *ifgfr2* or *ifgfr4* mRNA (\pm 1 μ M AP20187). AP20187 treatment was continuous from gastrula stage 10.5. Percentages of embryos from a representative experiment exhibiting the presented phenotype are indicated, iFgfr1, $n = 20$, iFgfr2 $n = 15$, iFgfr4, $n = 20$.

**Signalling by iFgfr1 and iFgfr2 regulates similar patterns of gene expression in gastrula stage embryos**

Our data indicate that *Fgfr1* and *Fgfr2* have similar abilities to activate MAP kinase ERK, and

ectopic signalling by either receptor results in rather similar phenotypic effects on development. We were interested to see if iFgfr1 and iFgfr2 signalling also results in similar effects on the early embryo transcriptome. Using the Affymetrix

microarray platform, we investigated changes in the transcriptome of embryos in which iFgfr1 and iFgfr2 signalling was activated from early gastrula stage 10.5 through to late gastrula stage 13.

Our expression analysis used sibling groups of control, iFgfr1 and iFgfr2-injected embryos. We adopted a strict filtering criterion of discarding data points if expression values of <50 FPKM were detected in both groups being compared (raw and filtered data sets are available in Supporting Information Spreadsheet 1). Scatterplots comparing \log_2 gene expression from these analyses are shown in Figure 4. Figure 4A is an analysis of expression levels in uninjected control embryos cultured either with or without AP20187. Of 10,958 probe sets passing the expression cut-off, we found that only six probe sets changed by more than or equal to twofold (4 up and 2 down) when AP20187 is added. This indicates culture in the presence of AP20187 had little effect on gene expression and, furthermore, at the expression cut-off levels employed, there was a high degree of congruence in gene expression between control groups. The high reproducibility between control groups is again demonstrated in Figure 4B, which compares gene expression in uninduced iFgfr1 and iFgfr2 groups. Of 10,794 genes passing the expression cut-off, only five probe sets differ by more than or equal to twofold (2 up and 3 down) between the two groups.

In contrast to the control groups, using ≥ 50 FPKM expression level cut-off, and more than or equal to twofold change criteria, we found that iFgfr1 and iFgfr2 activation resulted in differential expression of a number of genes. iFgfr1 activation upregulated 45 probe sets (Supporting Information Table 1) and downregulated 149 probe sets (Supporting Information Table 2). iFgfr2 activation upregulated 39 probe sets (Supporting Information Table 3) and downregulated 46 probe sets (Supporting Information Table 4).

The overlap between up and downregulated probe sets of uninduced versus induced iFgfr1 and iFgfr2 groups was investigated and is summarised in Supporting Information Spreadsheet 2 and the Venn diagram in Figure 4D. Whilst there are qualitative and quantitative differences in the effects of iFgfr1 and iFgfr2 activation on gene expression, it is striking that there are large overlaps between the regulated gene cohorts. Thus, of the 45 probe sets upregulated by iFgfr1, 56% were also upregulated by iFgfr2, and of the 39 probe sets upregulated by iFgfr2, 64%

were also upregulated by iFgfr1. Similarly, of the 149 probe sets downregulated by iFgfr1, 27% were also downregulated by iFgfr2, and of the 46 probe sets downregulated by iFgfr2, 87% were also downregulated by iFgfr1. Overall, our data support the notion that Fgfr1 and Fgfr2 regulate the expression of very similar cohorts of genes and this correlates with the similar effects resulting from their activation during gastrulation.

Previous transcriptomic studies of FGF signalling have involved inhibition or activation of FGF signalling from earlier blastula stages. Our study is designed to activate FGF signalling during a later time window towards the end of gastrulation, so we therefore expected to identify a cohort of FGF targets specifically regulated during this period. In addition to *egr1*, *cdx1*, *msx2*, *wnt8a* and *spry2*, which have been identified as being positively regulated by FGF signalling in previous *Xenopus* studies, we found both the nodal antagonist gene *lefty* and the *nek6* kinase gene to be upregulated by iFgfr1 and iFgfr2 which represent novel targets of FGF regulation at this later stage (Supporting Information Tables 1 and 3). In keeping with this, *T/brachyury* and *myod*, which are typically highly activated at the late blastula stage in the mesoderm, were only upregulated by 1.5- and 1.2-fold, respectively, in this data, and thus do not pass our strict selection criteria.

iFgfr1 and iFgfr4 signalling affects neural development

Previous studies have indicated that Fgfr1 and Fgfr4 signalling have differing effects on *Xenopus* neural development (Hongo et al., 1999; Hardcastle et al., 2000; Umbhauer et al., 2000). We investigated the effects of iFgfr1 and 4 signalling on neural development by targeted mRNA injection at the eight-cell stage into the two dorsal animal blastomeres, which are fated to make extensive contribution to the nervous system (Dale and Slack, 1987). iFgfr signalling was activated from gastrula stage 10.5 and phenotypic effects observed at larval stages. Figure 5A shows that activating iFgfrs in prospective neural tissue had less severe effects than when iFgfrs are expressed globally (Figure 3B). However, activation of either receptor caused defects in eye development. Activation of iFgfr1 signalling resulted in reduced retinal pigmentation and eye size, sometimes with the lens absent. In iFgfr4-induced embryos, the most

Figure 4 | See Legend on next page

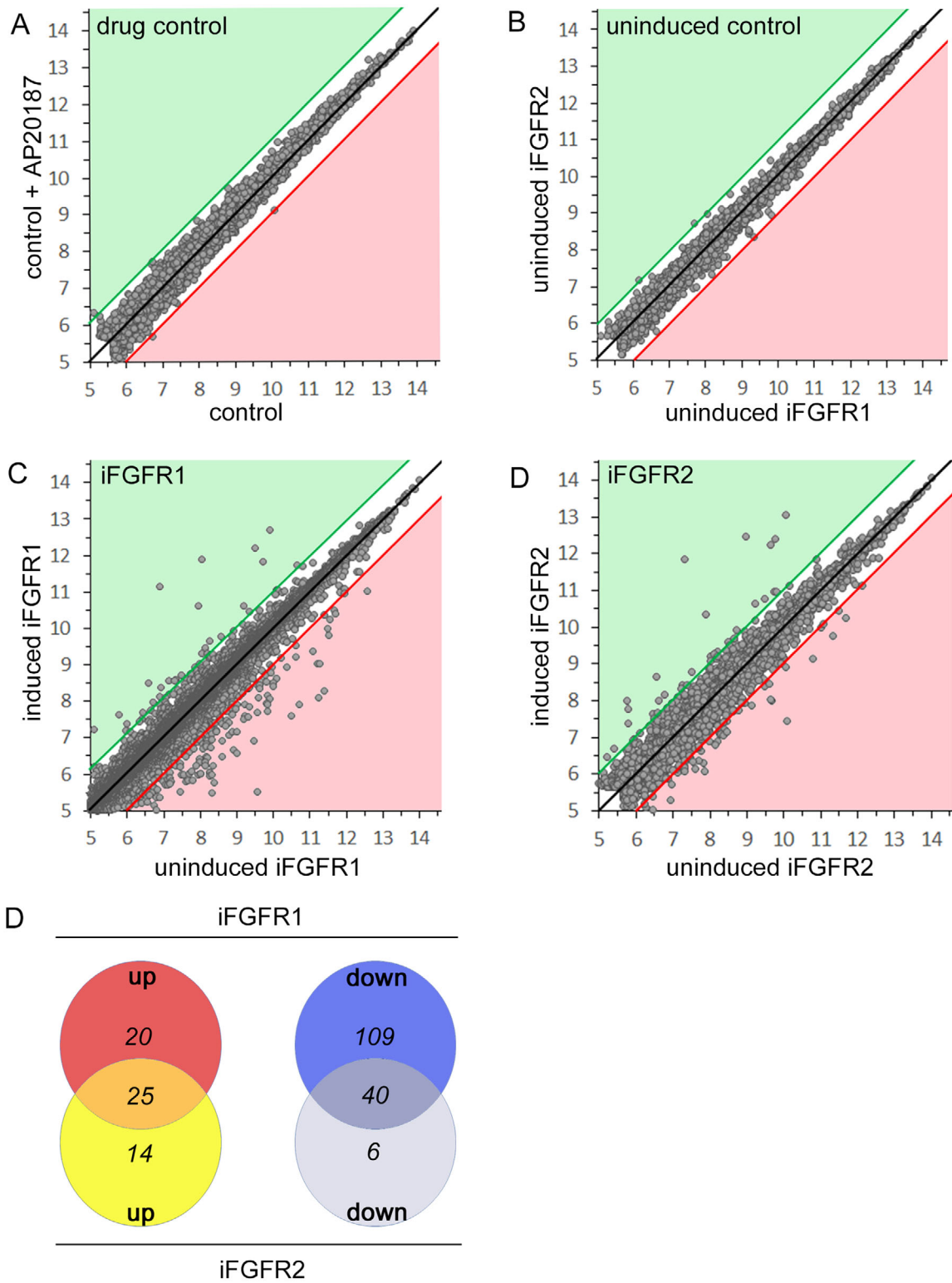


Figure 4 | Effects of iFgfr1 and iFgfr2 activation on the transcriptome of gastrula stage embryos

Scatterplots of \log_2 gene expression levels in late gastrula stage 13 embryos were generated using the Affymetrix microarray platform. Data were filtered with a cut-off to exclude array features with expression levels <50 . Data points in the white zone proximal to the black line ($y = x$) have less than twofold change in expression. Data points in the green zone have more than twofold increase in expression relative to control (x -axis). Data points in the red zone indicate more than twofold decrease in expression relative to control. Panel (A) compares gene expression in control uninjected embryos and uninjected embryos treated with $1 \mu\text{M}$ AP20187 from early gastrula stage 10.5. Panel (B) compares gene expression in embryos injected with 20pg *ifgfr1* or *ifgfr2* mRNA in the absence of AP20187 treatment (uninduced). Panels (C) and (D) compare gene expression in embryos injected with either 20pg iFgfr1 (C) or iFgfr2 mRNA (D) cultured in the absence (uninduced) or presence of $1 \mu\text{M}$ AP20187 from stage 10.5 (induced). Panel (E) is a Venn diagram showing the overlap of the gene sets up- and downregulated by more than or equal to twofold following activation of iFgfr1 and iFgfr2 signalling during gastrula stages.

common effect was missing pigmentation in parts of the retina. Previously, FGF signalling has been linked to eye development and regeneration in *Xenopus* and both *fgfr1* and *fgfr4* are expressed in the larval eye (Fukui and Henry, 2011; Kim et al., 2015). Deregulation of normal FGF signalling in the developing eye after iFgfr activation likely underpins the observed eye development defects observed in the current study.

iFgfr1 and iFgfr4 signalling activates MAP kinase signalling in neuralised ectoderm

To investigate the differing roles of *Fgfr1* and *Fgfr4* in regulating gene transcription during neural development we utilised the ability of the BMP inhibitor Noggin to neuralise animal caps explants, in combination with activation of iFgfr signalling. Our assay consisted of co-injecting *noggin* and *ifgfr* mRNAs into the early embryo. Animal caps were explanted at mid-blastula stage 8 and cultured until stage-matched control embryos reached early gastrula stage 10.5, at which point iFgfr signalling was induced for 3 h. Figure 5B is a western blot demonstrating that injection of *noggin* mRNA massively downregulated levels of phosphoSmad1/5/8 (pSmad1,5,8) (lane 3) compared to control animal caps (lane 4), indicating the effective inhibition of BMP signalling in animal cap explants, and this inhibition was not affected when iFgfr signalling was activated at the early gastrula stage (lane 7). Furthermore, the inhibition of BMP signalling did not compromise the ability of iFgfr signalling to activate MAP kinase signalling, as shown by levels of dp-ERK in non-neuralised animal caps (lane 5) versus neuralised animal caps (lane 7). Figure 5C shows that iFgfr4 signalling also upregulated dp-ERK levels, although, as previously

shown (Figure 2) the activation of MAP kinase signalling was less potent than seen with iFgfr1.

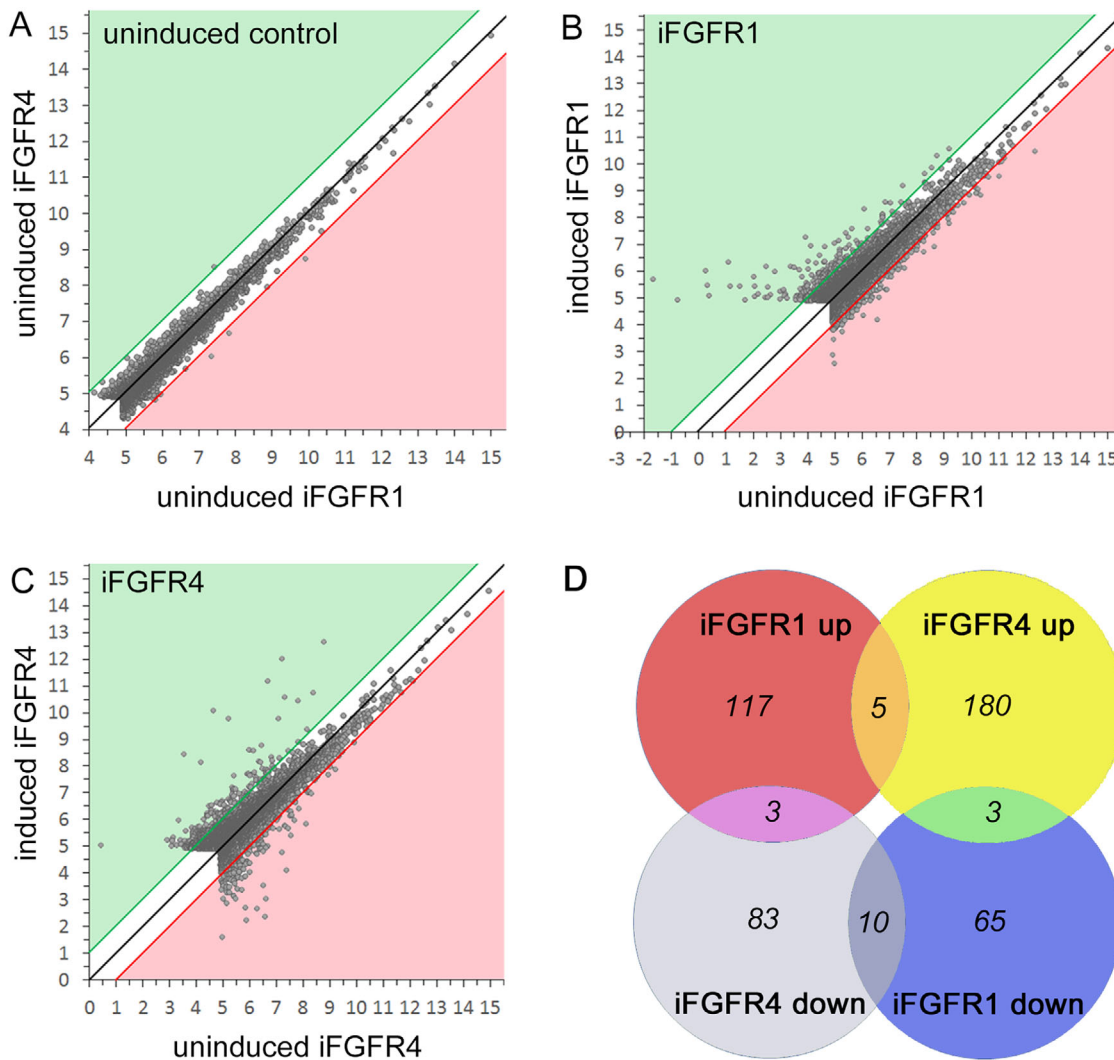
iFgfr1 and iFgfr4 signalling activates different patterns of gene expression in neuralised ectoderm

We used RNA-seq analysis to compare gene expression in Noggin-neuralised ectodermal explants and neuralised explants in which iFgfr1 or iFgfr4 signalling was induced at gastrula stage 10.5 for 3 hours. The rationale for using a short period of induction was to focus the analysis on proximal transcriptional events following activation of FGFR signalling. Animal cap explants from a sibling group of control, *ifgfr1* and *ifgfr4* injected embryos were analysed. Supporting Information Figure 2 shows a scatterplot comparing \log_2 unfiltered FPKM values for each annotated transcript model in uninduced iFgfr1 and iFgfr4 animal caps. There was considerable random variation in expression at the lower end of the dynamic range in this experiment. Therefore, a strict expression filter exclusion of <30 FPKM was adopted (raw and filtered data sets are available in Supporting Information Spreadsheet 3). Figure 6A shows that in the absence of AP20187, gene expression in *ifgfr1* and *ifgfr4* injected animal caps is very similar. A total of 6482 annotated transcripts were identified as passing the ≥ 30 expression cut-off criterion, and of these only five (1 up and 4 down) exhibited more than or equal to twofold change in expression. In contrast, a considerable number of transcripts were up and downregulated by induction of iFgfr signalling following the addition of AP20187.

A comparison between the iFgfr1 and iFgfr4 up and down regulated transcriptomes (Supplementary Tables 5, 6,7 and 8) contrasts with our analysis

Figure 6 | Effects of iFgfr1 and iFgfr4 activation on the transcriptome of neuralised tissue explants

Scatterplots of log₂ expression gene expression levels in neuralised animal cap explants generated from RNA-seq analysis data. Data were filtered with a cut-off to exclude identified gene models with expression levels <30 (FKPM). Data points in the white zone, proximal to the black line ($y = x$) have less than twofold change in expression. Data points in the green zone have a more than twofold increase in expression relative to control (x -axis). Data points in the red zone indicate more than twofold decrease in expression relative to control. Panel (A) compares gene expression in explants from embryos injected with 20 pg *ifgfr1* or *ifgfr4* mRNA in the absence of AP20187 treatment (uninduced). Panels (B) and (C) compare gene expression in explants from embryos injected with 20 pg *ifgfr1* (B) or *ifgfr4* mRNA (C) cultured in the absence (uninduced) or presence of 1 μM AP20187 from stage 10.5 for 3 h (induced). Panel (D) is a Venn diagram showing the overlap of gene sets up and down regulated by more than or equal to twofold following activation of iFgfr1 and iFgfr4 signalling in neuralised animal caps explants.



molecular function RNA binding (6.09x enrichment and 9.74×10^{-04}). In contrast, the cohorts of genes up and down regulated by iFgfr4 signalling showed no significant enrichment in slim molecular function terms using the same analysis.

It has been proposed that *Xenopus* Fgfr4 signalling is more strongly involved in neural development than Fgfr1 (Hongo et al., 1999; Hardcastle et al., 2000; Umbhauer et al., 2000). However, our analysis does not indicate enrichment of genes involved in neural

development regulated by *Fgfr4* signalling. In fact, we found that many genes associated with neural development, including the transcription factor genes *foxd4l1*, *bes1*, *foxb1*, *oct25*, *oct91* and *sp5l* were upregulated by *iFgfr1*, rather than *iFgfr4* signalling (Supplementary Spreadsheet 4). Despite this observation, there are indications that *Fgfr4* signalling is involved in cell lineage specification as we found that epidermal markers *krt5.7*, *tuba1a* and *xepsin* were strongly downregulated by *Fgfr4* signalling. A role for *Fgfr4* signalling in axial patterning was also indicated, as the anterior marker genes *hesx1*, *rax* and *otx2* are strongly downregulated by *iFgfr4* activation. This indicates that *Fgfr4* signalling likely contributes to the recognised role of FGF signalling in suppressing anterior and promoting posterior development (Cox Wm and Hemmati-Brivanlou, 1995; Lamb and Harland, 1995; Pownall et al., 1996; Polevoy et al., 2019).

Conclusion

We conclude that the use of timed activation of signalling by individual *iFgfrs* in whole embryos and within a specific tissue, neural in this case, provides a powerful tool for dissecting the role of FGF signalling in amphibian development. Our data show that *Fgfr1* and *Fgfr2* signalling have similar biological effects in the tissues of the early *Xenopus* embryo. We speculate that this is underpinned by the ability of both *Fgfr1* and 2 to robustly stimulate MAP kinase signalling. In contrast, *Fgfr4* only weakly activates MAP kinase signalling and has roles distinct from *Fgfr1* in regulating gene expression in developing amphibian neural tissue.

Materials and methods

iFgfr constructs

The CS2+ murine *iFgfr1* plasmid was PCR modified to remove the murine FGFR1 kinase domain sequence, generating a *Nhe1* restriction site downstream of the myristolation sequence and an *Mlu1* restriction site upstream of the sequence encoding the two AP20187 binding dimerisation domains. Sequences coding for the C-termini of *Xenopus laevis fgfr1*, 2,3 and 4 (accession number BC025936, BC073456, BC073428 and BC033318, respectively) were PCR amplified. In all cases the sequence amplified encoded the whole intracellular domain beginning four amino acids after the end of the transmembrane domain. During PCR amplification, 5' *Nhe1* and 3' *Mlu1* restriction sites were generated in each fragment. After restriction enzyme digest the kinase domain sequences were cloned in frame into the

Nhe1/Mlu1 site of the modified pCS+ vector. Each *iFgfr* protein was also tagged with a HA-epitope to allow monitoring of protein translation efficiency. Synthetic *iFgfr* mRNAs were produced from *Not1* linearised templates by *in vitro* transcription using the SP6 Megascript kit (Ambion) and a modified protocol using a 1:10 ratio of GTP to m7G(5')Gppp(5')G cap.

Embryological methods

Preliminary experiments (data not shown) were undertaken to determine optimal amounts of *iFgfr* mRNAs to inject and concentration of dimerising drug AP20187 to apply to injected tissues. Using *Xenopus laevis* embryos, we concluded that 20pg *iFgfr* mRNA minimised drug independent activation of FGFR signalling and exposure of tissues to 1 μ M AP20187 elevates the levels of activated diphospho-ERK (dp-ERK) in less than 15 min. This is in keeping with results obtained using an inducible murine FGFR1 (Pownall et al., 2003a). Embryos were injected with *iFgfr* mRNAs at the two-cell stage. For whole embryo experiments, *Xenopus laevis* embryos were cultured until stage 10.5 in NAM/3 +5% Ficoll and the treated with 1 μ M AP20187 [Clontech] in NAM/10 until late gastrula/early neurula stage 13. For animal cap experiments, embryos were co-injected with 20 pg *iFgfr* and 50 pg *noggin* mRNA into the animal pole at the one- to two-cell stage. Embryos were cultured until Stage 8 before transferring to a solution of NAM/2 and dissecting out ectodermal explants. Animal caps were cultured in NAM/2 until stage 10.5 and transferred to a 1 μ M solution of AP20187 in NAM/2 for 3 h. Embryos were staged according to Nieuwkoop and Faber (Nieuwkoop and Faber, 1967). Embryos were snap frozen or fixed at the required stage.

Western blotting and immunohistochemistry

Five *Xenopus laevis* embryos or >10 animal cap explants were homogenised in 50 μ L Phosphosafe (Novogen-Merk). Samples were analysed by SDS-PAGE and transferred onto Immobilon Millipore membrane (Fisher Scientific). Membranes were blocked in 5% milk powder in PBS and incubated overnight at 4°C in relevant primary antibodies (anti-dp-ERK (Sigma) 1:8000, anti-phosphoSmad1/5/8 (NEB) 1:500 and anti-GAPDH (HyTest) 1:1,000,000. Secondary antibodies were anti-mouse POD (Amersham), 1:3000 and anti-rabbit POD (Amersham), 1:2000. Signals were visualised with BM Chemiluminescence Western Blotting Substrate (POD) (Roche) and ECL Hyperfilm (Amersham). dp-ERK immunohistochemistry was carried out according to the methods of Christen and Slack (1999).

Transcriptomic analysis

Microarray analysis and RNA-seq analyses were carried on batches of RNA isolated from sibling embryos or explants from sibling embryos. Ten embryos or 20 animal caps were extracted in Tri-reagent (Sigma) according to the manufacturer's protocol. RNA for microarray analysis was precipitated using isopropanol and was further purified using Qiagen RNeasy columns, followed by a lithium chloride precipitation. RNeasy purification was omitted during the preparation of RNA for RNA-Seq analysis. Quality of purified total RNA was assessed using the Agilent 2100 Bioanalyzer. Two micrograms of total RNA was processed for Affymetrix microarray analysis using the Affymetrix GeneChip one-cycle target labelling kit (Affymetrix)

according to the manufacturer's recommended protocols. Processing of microarray samples was as per manufacturer's instructions and as previously described (Branney et al., 2009). Scanning and initial data processing were as previously described (Branney et al., 2009). Data were imported into BRB ArrayTools software (<http://linus.nci.nih.gov/BRB-ArrayTools.html>) for subsequent analysis.

RNA-seq samples were treated with Ribo-Zero rRNA Removal Kit (Illumina), generated cDNA was fragmented to 100–150 bp and sequenced on an Illumina HiSeq 2500 at the University of Liverpool Centre for Genomic Research. Approximately 110 million paired reads were obtained for iFgfr1 Uninduced, \approx 80 million for iFgfr1 Induced, \approx 90 million for iFgfr4 Uninduced and \approx 85 million reads iFgfr4 Induced. Raw Fastq files were trimmed for the presence of adapter sequences and reads shorter than 10 bp were removed. Mean read lengths after trimming were 82–96 bp and were aligned to the Mayball repository of *Xenopus laevis* longest cDNAs (<http://daudin.icmb.utexas.edu/>) using BWA-MEM (<http://bio-bwa.sourceforge.net/>; Li & Durbin 2009). Counts of reads per fragment mapping to each transcript were obtained by using SAMtools software (<http://samtools.sourceforge.net/>; Li et al. 2009). Initial analysis identified sequence hits for all models for individual genes. For subsequent analysis, multiple gene model hits were consolidated to single entry for each gene passing the filtering criteria. Threshold adjustment and genelist compiling, as well as further data analysis were performed in Microsoft Excel. Venn Diagrams were constructed using a tool on the University of Gent's Bioinformatics Evolutionary Genomics website (<http://bioinformatics.psb.ugent.be/webtools/Venn/>).

Animal usage

All animal work was undertaken with the approval of University of York ethics committees and in accordance with UK Home Office project licence POF245295.

Author contribution

H.B. undertook the experiments in this study and was involved in figure production and manuscript writing. H.V.I. conceived the project and was involved in figure production and manuscript writing.

Acknowledgments

We would like to thank Celina Whalley and Toby Hodges in the York Biology Technology Facility for their help with processing of the microarray and RNA-seq data. H.B. was in receipt of a BBSRC studentship.

Conflict of interest statement

The authors have declared no conflict of interest.

References

- Böttcher, R.T., Niehrs, C. and Bo, R.T. (2005) Fibroblast growth factor signaling during early vertebrate development. *Endocr. Rev.* **26**, 63–77
- Branney, P.A., Faas, L., Steane, S.E., Pownall, M.E. and Isaacs, H.V. (2009) Characterisation of the fibroblast growth factor dependent transcriptome in early development. *PLoS One* **4**, e4951
- Brewer, J.R., Mazot, P. and Soriano, P. (2016) Genetic insights into the mechanisms of Fgf signaling. *Genes Dev.* **30**, 751–771
- Carballada, R., Yasuo, H. and Lemaire, P. (2001) Phosphatidylinositol-3 kinase acts in parallel to the ERK MAP kinase in the FGF pathway during *Xenopus* mesoderm induction. *Development* **128**, 35–44
- Christen, B. and Slack, J. (1999a) Spatial response to fibroblast growth factor signalling in *Xenopus* embryos. *Development* **126**, 119–125
- Christen, B. and Slack, J.M. (1999b) Spatial response to fibroblast growth factor signalling in *Xenopus* embryos. *Development* **126**, 119–125
- Cox Wm, G. and Hemmati-Brivanlou, A. (1995) Caudalization of neural fate by tissue recombination and bFGF. *Development* **121**, 4349–4358
- Dale, L. and Slack, J.M.W. (1987) Fate map for the 32-cell stage of *Xenopus laevis*. *Development* **99**, 527–551
- Dorey, K. and Amaya, E. (2010) FGF signalling: diverse roles during early vertebrate embryogenesis. *Development* **137**, 3731–3742
- Fletcher, R.B., Baker, J.C. and Harland, R.M. (2006) FGF8 spliceforms mediate early mesoderm and posterior neural tissue formation in *Xenopus*. *Development* **133**, 1703–1714
- Fukui, L. and Henry, J.J. (2011) FGF Signaling Is Required for Lens Regeneration in *Xenopus laevis*. *The Biological Bulletin* **221**, 137–145
- Goldfarb, M. (2005) Fibroblast growth factor homologous factors: evolution, structure, and function. *Cytokine Growth Factor Rev.* **16**, 215–220
- Hardcastle, Z., Chalmers, A.D. and Papanalopulu, N. (2000) FGF-8 stimulates neuronal differentiation through FGFR-4a and interferes with mesoderm induction in *Xenopus* embryos. *Curr. Biol.* **10**, 1511–1514
- Hongo, I., Kengaku, M. and Okamoto, H. (1999) FGF signaling and the anterior neural induction in *Xenopus*. *Dev Biol* **216**, 561–581
- Isaacs, H.V., Pownall, M.E. and Slack, J.M. (1994) eFGF regulates Xbra expression during *Xenopus* gastrulation. *EMBO J.* **13**, 4469–4481
- Isaacs, H.V., Tannahill, D. and Slack, J.M.W. (1992) Expression of a novel FGF in the *Xenopus* embryo. A new candidate inducing factor for mesoderm formation and anteroposterior specification. *Development* **114**, 711–720
- Itoh, N. and Ornitz, D.M. (2008) Functional evolutionary history of the mouse Fgf gene family. *Dev Dyn.* **237**, 18–27
- Kim, Y.J., Bahn, M., Kim, Y.H., Shin, J.Y., Cheong, S.W., Ju, B.G., Kim, W.S. and Yeo, C.Y. (2015) *Xenopus laevis* FGF receptor substrate 3 (Xfrs3) is important for eye development and mediates Pax6 expression in lens placode through its Shp2-binding sites. *Dev. Biol.* **397**, 129–139
- LaBonne, C., Burke, B. and Whitman, M. (1995) Role of MAP kinase in mesoderm induction and axial patterning during *Xenopus* development. *Development* **121**, 1475–1486
- Lamb, T.M. and Harland, R.M. (1995) Fibroblast growth factor is a direct neural inducer, which combined with noggin generates anterior-posterior neural pattern. *Development* **121**, 3627–3636
- Li, H. and Durbin, R. (2009) Fast and accurate short read alignment with Burrows-Wheeler Transform. *Bioinformatics* **25**, 1754–1760
- Li, H., Handsaker, B., Wysoker, A., Fennell, T., Ruan, J., Homer, N., Marth, G., Abecasis, G. and Durbin, R. (2009) The Sequence

- Alignment/Map format and SAMtools. *Bioinformatics* **25**, 2078–2079
- Lombardo, A., Isaacs, H.V. and Slack, J.M. (1998) Expression and functions of FGF-3 in *Xenopus* development. *Int. J. Dev. Biol.* **42**, 1101–1107
- Nieuwkoop, P.D. and Faber, J. (1967) *Normal Table of Xenopus laevis (Daudin)*. Garland, Amsterdam
- Ornitz, D.M. and Itoh, N. (2015) The Fibroblast Growth Factor signaling pathway. *Wiley Interdiscip. Rev. Dev. Biol.* **4**, 215–266
- Ornitz, D.M., Xu, J., Colvin, J.S., McEwen, D.G., MacArthur, C.A., Coulier, F., Gao, G. and Goldfarb, M. (1996) Receptor specificity of the fibroblast growth factor family. *J. Biol. Chem.* **271**, 15292–15297
- Polevoy, H., Gutkovich, Y.E., Michaelov, A., Volovik, Y., Elkouby, Y.M. and Frank, D. (2019) New roles for Wnt and BMP signaling in neural anteroposterior patterning. *EMBO Rep.* **20**, 1–13
- Pownall, M.E. and Isaacs, H.V. (2010) *FGF Signalling in Vertebrate Development*. Biota, Princeton, NJ
- Pownall, M.E., Tucker, A.S., Slack, J.M.W. and Isaacs, H.V. (1996) eFGF, Xcad3 and Hox genes form a molecular pathway that establishes the anteroposterior axis in *Xenopus*. *Development* **122**, 3881–3892
- Pownall, M.E., Welm, B.E., Freeman, K.W., Spencer, D.M., Rosen, J.M. and Isaacs, H.V. (2003a) An inducible system for the study of FGF signalling in early amphibian development. *Dev. Biol.* **256**, 89–99
- Pownall, M.E., Welm, B.E., Freeman, K.W., Spencer, D.M., Rosen, J.M. and Isaacs, H.V. (2003b) An inducible system for the study of FGF signalling in early amphibian development. *Dev. Biol.* **256**, 89–99
- Raffioni, S., Thomas, D., Foehr, E.D., Thompson, L.M. and Bradshaw, R.A. (1999) Comparison of the intracellular signaling responses by three chimeric fibroblast growth factor receptors in PC12 cells. *Proc. Natl. Acad. Sci. U. S. A.* **96**, 7178–7183
- Session, A.M., Uno, Y., Kwon, T., Chapman, J.A., Toyoda, A., Takahashi, S., Fukui, A., Hikosaka, A., Suzuki, A., Kondo, M., van Heeringen, S.J., Quigley, I., Heinz, S., Ogino, H., Ochi, H., Hellsten, U., Lyons, J.B., Simakov, O., Putnam, N., Stites, J., Kuroki, Y., Tanaka, T., Michiue, T., Watanabe, M., Bogdanovic, O., Lister, R., Georgiou, G., Paranjpe, S.S., van Kruijsbergen, I., Shu, S., Carlson, J., Kinoshita, T., Ohta, Y., Mawaribuchi, S., Jenkins, J., Grimwood, J., Schmutz, J., Mitros, T., Mozaffari, S.V., Suzuki, Y., Haramoto, Y., Yamamoto, T.S., Takagi, C., Heald, R., Miller, K., Haudenschild, C., Kitzman, J., Nakayama, T., Izutsu, Y., Robert, J., Fortriede, J., Burns, K., Lotay, V., Karimi, K., Yasuoka, Y., Dichmann, D.S., Flajnik, M.F., Houston, D.W., Shendure, J., DuPasquier, L., Vize, P.D., Zorn, A.M., Ito, M., Marcotte, E.M., Wallingford, J.B., Ito, Y., Asashima, M., Ueno, N., Matsuda, Y., Veenstra, G.J., Fujiyama, A., Harland, R.M., Taira, M. and Rokhsar, D.S. (2016) Genome evolution in the allotetraploid frog *Xenopus laevis*. *Nature* **538**, 336–343
- Sivak, J.M., Petersen, L.F. and Amaya, E. (2005) FGF signal interpretation is directed by Sprouty and Spred proteins during mesoderm formation. *Dev. Cell* **8**, 689–701
- Slack, J.M., Darlington, B.G., Heath, J.K. and Godsave, S.F. (1987) Mesoderm induction in early *Xenopus* embryos by heparin-binding growth factors. *Nature* **326**, 197–200
- Slack, J.M.W., Isaacs, H.V. and Darlington, B.G. (1988) Inductive effects of fibroblast growth factor and lithium ion on *Xenopus* blastula ectoderm. *Development* **103**, 581–590
- Song, J. and Slack, J.M.W. (1996) The cloning of *Xenopus* FGF-9. *Dev. Dyn* **206**, 427–436
- Suzuki, A., Yoshida, H., van Heeringen, S.J., Takebayashi-Suzuki, K., Veenstra, G.J.C. and Taira, M. (2017) Genomic organization and modulation of gene expression of the TGF-beta and FGF pathways in the allotetraploid frog *Xenopus laevis*. *Dev. Biol.* **426**, 336–359
- Umbhauer, M., Penzo-Méndez, a., Clavilier, L., Boucaut, J. and Riou, J. (2000) Signaling specificities of fibroblast growth factor receptors in early *Xenopus* embryo. *J. Cell Sci.* **113(Pt 1)**, 2865–2875
- Welm, B.E., Freeman, K.W., Chen, M., Contreras, A., Spencer, D.M. and Rosen, J.M. (2002) Inducible dimerization of FGFR1: development of a mouse model to analyze progressive transformation of the mammary gland. *J. Cell Biol.* **157**, 703–714
- Yamagishi, M. and Okamoto, H. (2010) Competition for ligands between FGFR1 and FGFR4 regulates *Xenopus* neural development. *Int. J. Dev. Biol.* **54**, 93–104

Received: 18 October 2019; Revised: 31 January 2020; Accepted: 31 January 2020; Accepted article online: 6 February 2020